Organic & Biomolecular Chemistry

Insertion of a methylene group into the backbone of an antisense oligonucleotide reveals importance of deoxyribose recognition by RNase H

Journal:	*Organic & Biomolecular Chemistry*
Manuscript ID	OB-ART-09-2022-001667.R1
Article Type:	Paper
Date Submitted by the Author:	19-Oct-2022
Complete List of Authors:	Masaki, Yoshiaki; Tokyo Institute of Technology, Department of Life Science and Technology; Japan Science and Technology Agency, PRESTO Tabira, Ayano; Tokyo Institute of Technology, Department of Life Science and Technology Hattori, Shihori ; Tokyo Institute of Technology, Department of Life Science and Technology Wakatsuki, Shunsuke ; Tokyo Institute of Technology, Department of Life Science and Technology Seio, Kohji; Tokyo Institute of Technology, Life Science and Technology

ARTICLE

Insertion of a methylene group into the backbone of an antisense oligonucleotide reveals importance of deoxyribose recognition by RNase H

Received 00th January 20xx,
Accepted 00th January 20xx

DOI: 10.1039/x0xx00000x

Yoshiaki Masaki,[a,b*] Ayano Tabira,[a] Shihori Hattori,[a] Shunsuke Wakatsuki,[a] Kohji Seio[a]

RNase H acts as a key effector in gene knockdown by antisense oligonucleotides (ASOs). Although various chemical modifications have been developed to regulate RNase H-mediated cleavage, precise control is yet to be achieved. In this study, we tried to address the question whether the interaction of phosphate groups or deoxyriboses is more important in the recognition of DNA/RNA duplex by RNase H. To answer this question, we investigated the effect of methylene group insertion at the 5′-upstream or 3′-downstream phosphorothioate groups on RNase H-mediated cleavage. By inserting a methylene group at the 5′-upside or 3′-downside, the distance between phosphates or deoxyriboses could be changed in a different pattern. Maximum suppression of the cleavage reaction was observed when a methylene group was inserted at the 5′-phosphate group of the nucleoside which is known to distinguish ribose and deoxyribose via stacking of the W221 residue in RNase H. This effect was observed in a different sequence as well as mismatched duplexes, suggesting the interaction of deoxyribose rings with RNase H is more important than that of phosphate groups. Our results will contribute to the designing of further molecular modifications that improve the selectivity of RNase H-mediated cleavage reactions which allows for the development of allele-specific ASOs.

Introduction

RNase H is an endogenous nuclease that recognizes DNA/RNA duplexes and exclusively cleaves the RNA strand.[1] Because RNase H is ubiquitously expressed, a short synthetic DNA molecule, also termed as antisense oligonucleotide (ASO), can be used as a catalyst to degrade RNA with a complementary sequence. This mechanism has been widely used, not only as a biological tool but also for therapeutic purposes.[2–4] To improve the nuclease resistance, duplex stability and distribution of ASOs, various kinds of chemical modifications have been developed.[5–9] Although RNase H preferentially binds and cleaves fully complementary DNA/RNA duplexes, it is known that DNA/RNA duplexes containing mismatches or bulges could also act as substrates for RNase H.[10] This low selectivity makes it difficult to develop allele-specific ASOs. In addition, the development of safer ASOs involves potential hurdles. Altering the position of RNase H-mediated cleavage via chemical modifications appears to be a promising technique that may be used to overcome these hurdles.

Nowotny *et al*. revealed the X-ray structure of human RNase H1 catalytic domain-DNA/RNA.[11] In this structure, the phosphate group of the DNA strand was recognized by multiple

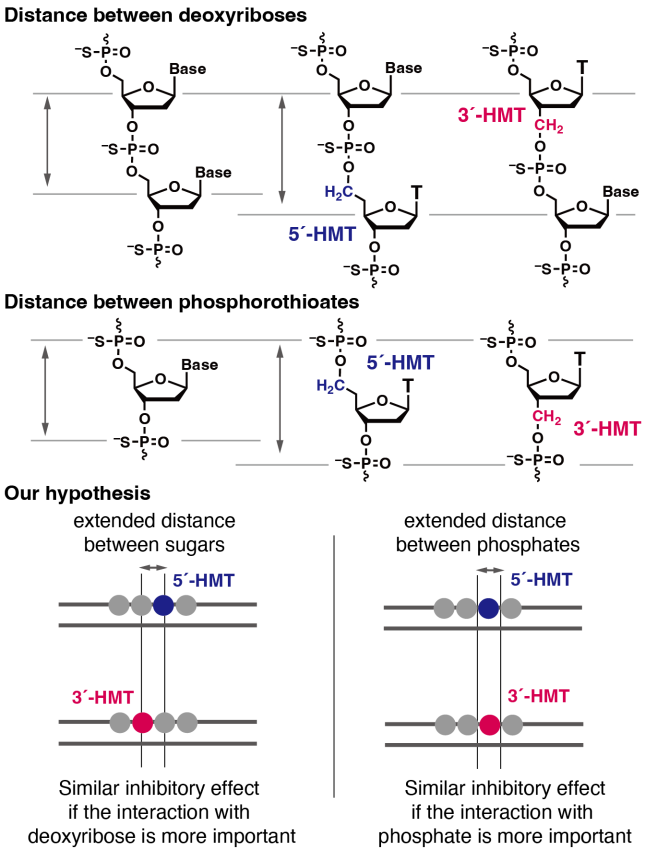

Fig. 1 Insertion of methylene group in phosphorothioate backbones.

[a] *Department of Life Science and Technology, Tokyo Institute of Technology, 4259-J2-16 Nagatsuta, Midori, Yokohama, Kanagawa, 226-8501, JAPAN.*
[b] *PRESTO, JST, 4-1-8 Honcho, Kawaguchi, Saitama, 332-0012, JAPAN.*
† Footnotes relating to the title and/or authors should appear here.
Electronic Supplementary Information (ESI) available: [details of any supplementary information available should be included here]. See DOI: 10.1039/x0xx00000x

amino acid residues, especially R179, T181, and N240, which form hydrogen bonds with a single phosphate group. The space formed by these amino acid residues is termed the phosphate-binding pocket. In addition to the phosphate-binding pocket two neighboring 3′-downstream phosphate groups have been recognized via multiple interactions, suggesting that phosphate modification near these positions may enable the position of RNase H-mediated cleavage to be controlled. Iwamoto et al., reported that the incorporation of stereo-pure R or S-phosphorothioate enhanced RNase H-mediated cleavage.[12] In addition, phosphate backbone modifications, such as alkyl phosphonate linkage, 5′-alkyl modification,[13] alkylphosphonate linkage,[14] mesyl-phosphoramidate linkage,[15] and boranophosphate,[16] have been shown to influence the cleavage pattern of RNase H. In addition to phosphate backbone modifications, sugar modifications have also reportedly changed preferences for RNase H-DNA/RNA complex formation.[17–23]

Our question was whether the interaction of phosphate groups or deoxyribose rings is more important in the recognition of DNA/RNA duplex by RNase H. To answer this question, we focused on the effect exerted by a methylene group that is inserted into the phosphate backbone. By inserting a methylene group at the 5′-upside or 3′-downside, the distance between phosphates or deoxyribose rings could be changed in a different pattern (Figure 1). Our hypothesis is if interactions with deoxyribose rings were more important, we expected to observe the largest inhibition effect when the distance between the same deoxyribose rings was elongated. Similarly, if interactions with phosphate groups were more important, we expected to observe the largest inhibition effect when the distance between the same phosphate groups was elongated.

In this study, we investigated the effect of inserting a methylene group into the phosphorothioate backbone on RNase H-mediated cleavage. The syntheses of 5′-deoxy-5′-*C*-(hydroxymethyl)thymidine (5′-HMT) and 3′-deoxy-3′-*C*-(hydroxymethyl)thymidine, which have extended backbones with a methylene group, have been previously reported.[24] We introduced these modifications into ASOs and evaluated RNase H-mediated cleavage patterns of modified ASOs with complementary RNA. In addition, the effect of positional modification on the RNase H-DNA/RNA complex and its applicability to mismatched duplexes were evaluated.

Results and discussion

We synthesized 5′-deoxy-5′-*C*-(hydroxymethyl) thymidine (5′-HMT) and its phosphoramidite derivative using a procedure previously reported by Kofoed et al.[24] Although the synthesis was completed smoothly, the solubility of the purified phosphoramidite derivative in acetonitrile was unexpectedly poor. Therefore, we introduced a benzoyl group at the *N*-3 position. The scheme for the synthesis of benzoyl-protected phosphoramidite derivatives is shown in the Supporting Information (Scheme S1). The benzoyl-protected phosphoramidite derivative dissolved well in acetonitrile and could be applied to a DNA auto-synthesizer. For 3′-deoxy-3′-*C*-(hydroxymethyl)thymidine (3′-HMT), the nucleoside was synthesized via a method reported by Sanghevi et al.[25] Next, the nucleoside was converted to the corresponding phosphoramidite derivative via the procedure reported by Kofoed et al.[24]

Table 1. ASO sequences targeting Huntingtin (*HTT*) mRNA

	Sequence[a]	cacld.	found
Control	5′-TAA-attgtcatc-ACC	4961.0	4961.0
5′-HMT-2	5′-TAA-a**X**tgtcatc-ACC	4975.1	4975.8
5′-HMT-3	5′-TAA-at**X**gtcatc-ACC	4975.1	4976.0
5′-HMT-5	5′-TAA-attg**X**catc-ACC	4975.1	4975.4
5′-HMT-8	5′-TAA-attgtca**X**c-ACC	4975.1	4975.7
3′-HMT-2	5′-TAA-a**Y**tgtcatc-ACC	4975.1	4975.2
3′-HMT-3	5′-TAA-at**Y**gtcatc-ACC	4975.1	4975.6
3′-HMT-5	5′-TAA-attg**Y**catc-ACC	4975.1	4974.9
3′-HMT-8	5′-TAA-attgtca**Y**c-ACC	4975.1	4975.2

[a] Capital letters denote locked nucleic acid (LNA). Small letters denote the DNA. X and Y denote 5′-deoxy-5′-*C*-(hydroxymethyl)thymidine and 3′-deoxy-3′-*C*-(hydroxymethyl)thymidine, respectively. All phosphate groups were phosphorothioates. All the cytosine bases were 5-methylated.

Table 2. Melting temperatures of the HTT targeting ASOS-RNA duplexes.[a]

	5′-r(GGUGA-x-GACAAUUUA)				ΔT_m[b]
	PM (x = rA)	**MM** (x = rG)	x = rC	x = rU	
control	55.8±1.6	54.4±0.7	44.0±0.3	47.4±0.5	−1.4
5′-HMT-2	53.8±1.2	51.9±0.6	40.6±0.3	44.8±0.6	−1.9
5′-HMT-3	56.1±1.0	54.4±0.7	43.8±0.1	47.1±0.4	−1.7
5′-HMT-5	57.2±0.8	55.1±0.7	45.1±0.3	48.3±0.5	−2.0
5′-HMT-8	56.8±1.3	55.4±0.7	45.3±0.3	48.4±0.6	−1.3
3′-HMT-2	53.0±0.7	52.1±0.7	40.2±0.3	45.4±0.6	−0.9
3′-HMT-3	54.6±0.7	53.1±0.6	41.2±0.5	47.2±0.6	−1.6
3′-HMT-5	54.2±0.8	53.4±0.7	43.2±0.5	46.8±0.7	−0.8
3′-HMT-8	53.9±0.6	52.8±0.7	41.3±0.4	46.1±0.5	−1.1

[a] The unit is °C. [b] ΔT_m is the smallest difference between the T_m values of perfectly matched RNA (PM, x = rA) with ASO and mismatched RNA (MM, x = rG) with ASO.

The synthesized ASOs are listed (Table 1). The ASO sequence targets a mutant huntingtin (HTT) mRNA.[18,19,26] In the previous study, the combination of 2′-*O*-methoxyethyl (MOE) and 2′,4′-constrained-[S]-2′-*O*-ethyl (S-cEt) modified nucleotides were used for the wing region. To mimic their ASOs, we used locked nucleic acid (LNA) instead of MOE and S-cEt. For the ASO names, numbering denotes the position of modification from the 5′-side in the DNA gap region. For example, **5′-HMT-2** indicates that a 5′-HMT modification was introduced into the second position in the DNA gap region. Similarly, **5′-HMT-3**, **5′-HMT-5**, and **5′-HMT-8** indicate 5′-HMT modifications at the third, fifth, and eighth positions, respectively. **3′-HMT-2**, **3′-HMT-3**, **3′-HMT-5**, and **3′-HMT-8** represent 3′-HMT modifications at the

second, third, fifth, and eighth positions, respectively. The coupling reaction of modification was performed twice with an extended coupling time of 12 min, for precaution; 5-(Benzylthio)-1*H*-tetrazole was used as an activator and ((dimethylamino-methylidene)amino)-3*H*-1,2,4-dithiazoline-3-thione (DDTT) was used as the sulfurizing reagent. Synthesized ASOs were purified using reversed-phase HPLC and confirmed using matrix-assisted laser desorption ionization time-of-flight mass spectrometry (Figure S1).

To investigate the effect of modifications on duplex stability, UV-melting analysis of modified ASOs with complementary RNA 5′-r(GGUGA-x-GACAAUUUA), where x = rA, rG, rC, or rU was performed (Table 2, Figure S2). The position of x, opposite T, in ASO corresponds to the single-nucleotide polymorphism (SNP, dbSNP Reference SNP number: rs7685686, G/A), which reportedly allow disease-specific targeting of HTT.[26] In addition to the SNP combination, we also evaluated other mismatched base pairings. The melting temperature (T_m) of the °control with complementary RNA (**PM**: x = rA) was 55.8 ± 1.6°C. Similarly, the T_ms of **5′-HMT-2**, **5′-HMT-3**, **5′-HMT-5**, and **5′-HMT-8** with the **PM** were 53.8 ± 1.2°C, 56.1 ± 1.0°C, 57.2 ± 0.8°C, 56.8 ± 1.3°C, respectively. The T_ms of **3′-HMT-2**, **3′-HMT-3**, **3′-HMT-5**, and **3′-HMT-8** with the **PM** were 53.0 ± 0.7°C, 54.6 ± 0.7°C, 54.2 ± 0.8°C, 53.9 ± 0.6°C, respectively. Surprisingly, 5′-HMT modification showed almost identical T_m values to the control experiment, except for **5′-HMT-2**. It has been reported that 5′-HMT and 3′-HMT modifications destabilize the 14-mer DNA duplex by approximately −3°C.[24] Because the ASO-RNA duplex was expected to form a structure different from that of the B-type DNA duplex, it was expected to accept the extended phosphorothioate backbone rather than the DNA duplex.

The T_m of the control with a mismatched (**MM**) RNA (x =rG) was 54.4 ± 0.7°C, which was higher than those of the other mismatches (x = rC (44.0 ± 0.3°C) or x = rU (47.4 ± 0.5°C)). Base recognition ability (ΔT_m) was calculated as the difference between the T_m value of the control duplex and that of the highest mismatched duplex. For the control, ΔT_m was −1.4°C. Similarly, the ΔT_m of **5′-HMT-2**, **5′-HMT-3**, **5′-HMT-5**, and **5′-HMT-8** with the **PM** were −1.9°C, −1.7°C, −2.0°C, and −1.3°C, respectively. The T_m of **3′-HMT-2**, **3′-HMT-3**, **3′-HMT-5**, and **3′-HMT-8** with the **PM** were −0.9°C, −1.6°C, −0.8°C, and −1.1°C, respectively. Base recognition ability was retained even after the 5′-HMT or 3′-HMT modification was introduced.

To understand the impact of the insertion of a methylene group on the cleavage reaction, we analyzed RNase H-mediated RNA cleavage by ASOs duplexed with the above complementary RNA (**PM**; Figure 2). The cleavage reaction was performed using commercially available RNase H from Escherichia coli, which is often used to model the human RNase H catalytic domain.[10,20] It has been reported that the cleavage pattern of the human RNase H1 catalytic domain resembles that of E. coli RNase H.[27] We also confirmed that the cleavage pattern observed using E. coli RNase H (Figure 2A) resembled the cleavage pattern reportedly observed using human RNase H1.[19] The cleavage of **PM** in the presence of each ASO yielded five products, denoted as cleavage products ***a***, ***b***, ***c***, ***d***, and ***e***, in different ratios (Figure 2B). Here, ***a***–***e*** were as follows: 5′-FAM-r(GGUGAUGA); 5′-FAM-r(GGUGAUGAC); 5′-FAM-r(GGUGAUGACA); 5′-FAM-r(GGUGAUGACAA); and 5′-FAM-r(GGUGAUGACAAU), respectively. Qualitatively, the most significant differences were observed in the cases of **5′-HMT-8** and **3′-HMT-5**, in which the dominantly observed the cleavage products ***a*** and ***c*** in control, respectively, were suppressed. Quantitative analyses were performed to analyze the data in more detail.

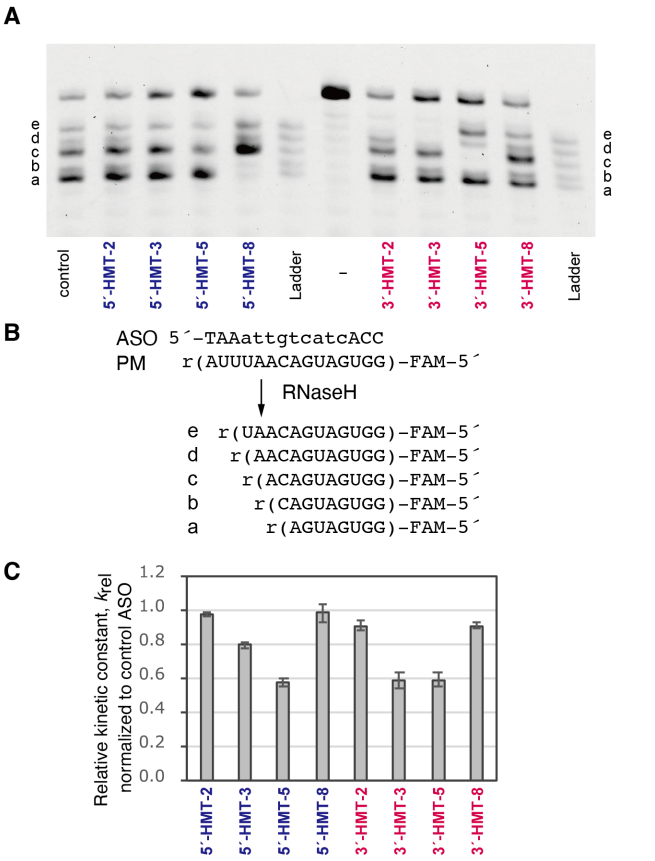

Fig. 2 RNase H-mediated cleavage patterns of ASO/PM duplexes. (A) Electrophoretic mobility shift assay of RNase H mediated cleavage products. A mixture of synthetic FAM-labelled RNAs was used as a ladder. (B) Expected cleavage products. (C) Kinetic constants (k_{rel}) of cleavage by a modified ASO relative to a control ASO. Error bars (standard deviation) were calculated from three independent experiments.

First, the initial velocity of RNA cleavage was estimated. The reactions were quenched after 5 min, and assuming first-order kinetics, the relative kinetic constants (k_{rel}) of ASOs for the control were calculated from the residual RNA fractions (Figure 2C); (See derivation in supporting information).

$$k_{rel} = \frac{ln(f_{RNA\_m})}{ln(f_{RNA\_C})}$$

where f_{RNA_m} is the residual **PM** fraction in the experiment using the modified ASO/**PM** duplex and f_{RNA_C} is the fraction of the residual **PM** in the experiment using the control/**PM** duplex. The k_{rel} of **5′-HMT-2** was 0.98 ± 0.01, indicating that **5′-HMT-2** showed a cleavage rate comparable to that of the control as far as the consumption of **PM** was considered. Similarly, the k_{rel} of

5′-HMT-3, **5′-HMT-5**, and **5′-HMT-8** were 0.79 ± 0.02, 0.57 ± 0.02, and 0.98 ± 0.05, respectively; **5′-HMT-3** and **5′-HMT-5** showed slower cleavage rates than the control. The k_{rel} of **3′-HMT-2**, **3′-HMT-3**, **3′-HMT-5**, and **3′-HMT-8** were 0.90 ± 0.03, 0.58 ± 0.05, and 0.58 ± 0.04, and 0.91 ± 0.02, respectively. Here, **3′-HMT-2** and **3′-HMT-8** slightly decreased the overall cleavage rate, whereas the rates of **3′-HMT-3** and **3′-HMT-5** decreased. In order to understand these differences, we focused on cleavage products.

The control yielded five cleavage products, named ***a***, ***b***, ***c***, ***d***, and ***e***, in which ***a*** and ***c*** were the most and the second most abundant, respectively. Each cleavage product was supposed to result from the cleavage reaction of the RNase H-ASO/RNA complex at different sequence positions. To elucidate the influence of modifications on cleavage patterns, we analyzed the position of each modification relative to the nucleoside residue recognizing the cleavage site. The relative positions of the modifications overwritten in the human RNase H1 catalytic domain-DNA/RNA structure (PDB: 2QK9) are shown (Figure 3A). Position **0** was defined as the deoxynucleotide that recognized the cleavage site. The nucleotide 5′-upstream to position **0** is defined as position **−1**, and the nucleotide 3′-downstream as position **+1**. Based on the X-ray structure of sugars in DNA (ASO in the case of the current study) at positions **0**, **+1**, **+2**, **+3**, and **+4** were in close contact with RNase H. The nucleobases of DNA at positions **−1** and **+5** were also close to RNase H. Examples of the relationships between the cleavage product and the relative position of the modification are shown (Figure 3C).

In **5′-HMT-2**, cleavage product ***c*** is the result of cleavage when the modification is at position **−1** in the complex (Figure 3C). Similarly, the cleavage products *c* in **5′-HMT-3**, **5′-HMT-5**, and **5′-HMT-8** were the products when the modification is at positions **0**, **+2**, and **+5**, respectively. The conversion table of the cleavage products to the relative positions of the modifications is shown (Figure 3D). Using this description, the cleavage pattern of **5′-HMT-8**, via which the cleavage to product ***a*** was suppressed, suggested that the 5′-HMT modification disfavored position **+3**. Similarly, the pattern for **3′-HMT-5**, by which the cleavage to product ***c*** was suppressed, suggested that the 3′-HMT modification disfavored position **+2**.

To make this discussion more quantitatively, the positional relative kinetic constants (k_{rel_i}) were defined as the indicator of the velocity of the cleavage when the modification is at position *i*. To calculate k_{rel_i}, we approximated the cleavage reaction as a parallel pseudo-first-order reaction. Under this assumption, k_{rel_i} can be expressed by following equation (See derivation in supporting information).

$$k_{rel\_i} = \frac{p_{m\_i}}{p_{c\_i}} k_{rel}$$

where p_{m_i} is the fraction of the cleavage product obtained using the modified ASO when the modification occurred at position i. p_{c_i} is the fraction corresponding to p_{m_i} of the cleavage product obtained using the control. Briefly, in each lane (Figure 2B), the fluorescence intensities of the bands corresponding to products ***a***–***e*** were measured. Then, the fraction *p* of each cleavage product was calculated by dividing the fluorescence intensity of the product band by the sum of the fluorescence intensities of cleavage products that did not include the remaining intact RNA. Subsequently, considering the differences in the cleavage rates among the lanes shown (Figure 2), the ratio of cleavage product fraction *p* between modified ASOs and the control was

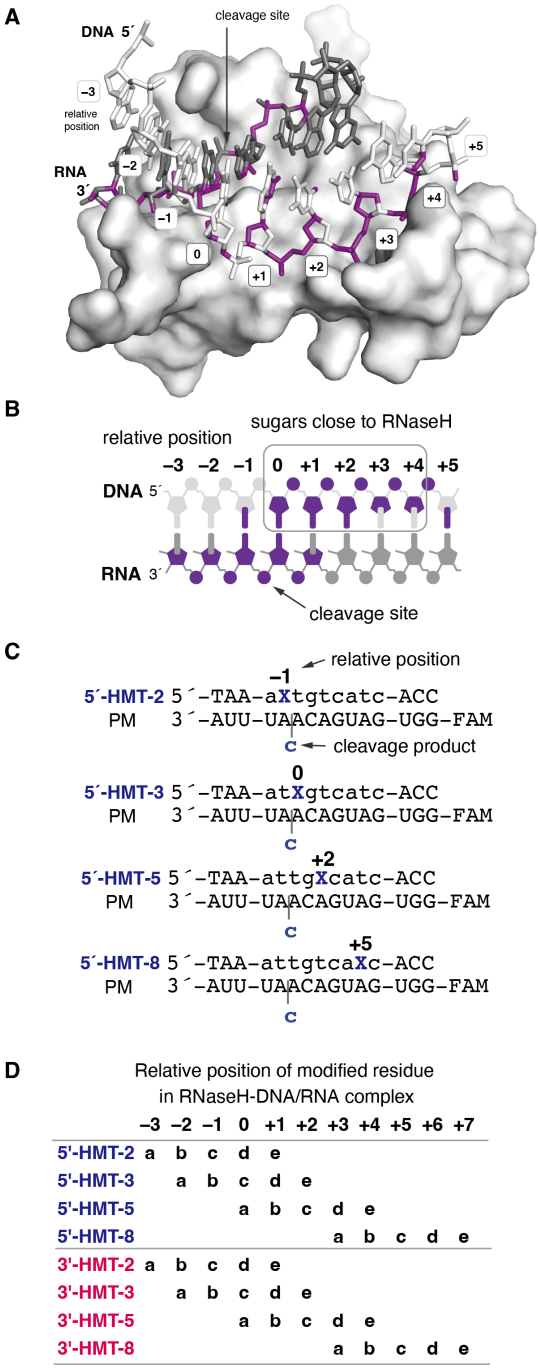

	−3	−2	−1	0	+1	+2	+3	+4	+5	+6	+7
5′-HMT-2	a	b	c	d	e						
5′-HMT-3		a	b	c	d	e					
5′-HMT-5				a	b	c	d	e			
5′-HMT-8							a	b	c	d	e
3′-HMT-2	a	b	c	d	e						
3′-HMT-3		a	b	c	d	e					
3′-HMT-5				a	b	c	d	e			
3′-HMT-8							a	b	c	d	e

Fig. 3 Definition of relative positions in the RNase H-DNA/RNA complex. (A) X-ray structure of human RNase H1 catalytic domain-DNA/RNA complex (PDB: 2QK9). The atoms close to RNase H1 within 4 Å are colored purple. (B) Diagram of relative position and cleavage site. The moieties close to RNase H1 are colored purple. (C) Examples of conversion from cleavage product to the relative positions of a modified residue in each ASO. (D) Relationship of cleavage product and relative position of modified residue in each ASO.

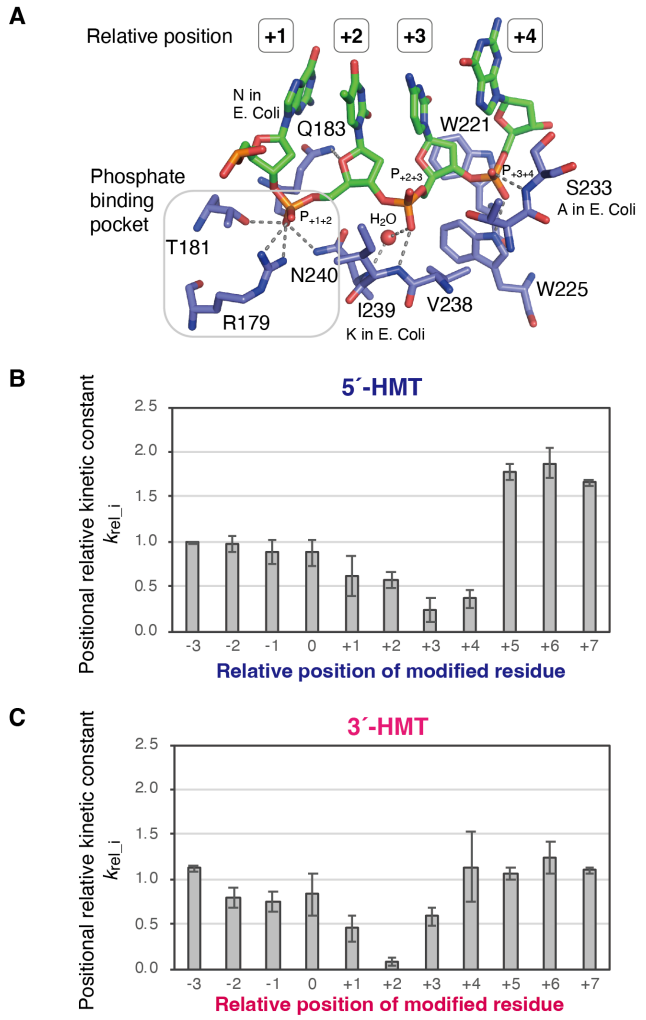

Fig. 4 Effect of modified residue on positional relative kinetic constants. Error bars denote standard deviations calculated from three independent experiments. (A) Interaction between the DNA strand and amino acid residues in RNase H (PDB: 2QK9). (B) Positional relative kinetic constants (k_{rel_i}) of 5´-HMT modification. (C) The k_{rel_i} of 3´-HMT modification. For the purpose of assessing quantitative aspects, the k_{rel_i} was defined as an indicator of the velocity of cleavage when modification occurred at position i. To calculate k_{rel_i}, we approximated the cleavage reaction to a parallel pseudo-first-order reaction. (derivation is presented in supporting information).

multiplied by the k_{rel} described above. For **5´-HMT-2**, the calculated values form ***a***-***e*** bands were assigned to k_{rel_-3} and k_{rel_+1}, respectively (Figure 3D). For example, k_{rel_0} was calculated using the fractions of product ***d*** in **5´-HMT-2**, product ***c*** in **5´-HMT-3**, and product ***a*** in **5´-HMT-5**. Thus, the average values of these three data points were used for k_{rel_0}. Using all k_{rel_i} thus calculated, the positional effect of the modification can be quantitatively assessed. As shown in Table S1 and S2, the positional effect among differently modified ASOs were similar. For the 5´-HMT modification at position **-3**, the calculated k_{rel_-3} was 0.99 ± 0.01, suggesting almost no influence on the cleavage reaction. The minimum k_{rel_i} was observed at position **+3** (0.23 ± 0.13), which agreed with the qualitative observation in **5´-HMT-8**. Similarly, in the case of 3´-HMT modification, the minimum k_{rel_i} was observed at position **+2** (0.08 ± 0.04), which was also in agreement with the qualitative observation in **3´-HMT-5**.

In human RNase H, the phosphate group between positions **+1** and **+2** (P_{+1+2}) is recognized by three amino acids (R179, T181, and N240), also described as the phosphate-binding pocket, which is a conserved amino acid residue in E. coli. In addition to P_{+1+2}, the phosphate groups (P_{+2+3} and P_{+3+4}) also formed hydrogen bonds with amide groups in the main chain of RNase H and the amide group of the conserved amino acid, W225 (Figure 4A; Figure S3A). Here, 5´-HMT at position **+3** indicates that the methylene group was inserted at P_{+2+3}, while the 3´-HMT at position **+2** indicates methylene group insertion at P_{+2+3}.

In the case of 5´-HMT at **+3** position, the phosphate between P_{+2+3} and P_{+3+4} is elongated by a methylene group. If this phosphates elongation is important, 3´-HMT at **+3** position should be largely suppressed for the same reason. Similarly, in the case of 3´-HMT at **+2** position, the phosphate between P_{+1+2} and P_{+2+3} is elongated by a methylene group. If this is the case, 5´-HMT at **+2** position should be suppressed. But in both cases, 3´-HMT at **+3** and 5´-HMT at **+2** position, the inhibitory effect was not strong. In the X-ray crystal structure (PDB: 2QK9), the distance between P_{+1+2} and P_{+2+3} was 7.2 Å, which is longer than that between P_{+2+3} and P_{+3+4} (6.2 Å), suggesting the methylene insertion at **+2** position might be accepted than the other positions. In contrast to this structural suggestion, the 3´-HMT at **+2** position significantly suppressed the cleavage reaction in our study. These considerations suggested that the elongation of phosphate groups was not the main reason for the large suppression by a methylene insertion.

The effect of methylene insertion is not only the distance elongation but also local conformational change. It is reported that RNase H interactions generate a local distortion to facilitate protein binding.[28] We assumed the methylene insertion could lead to the more flexible conformation due to the lack of gauche effect between the phosphate group and the O4' atom. But if this flexibility is important, the strongest effect by 5´-HMT and 3´-HMT would be observed in the same position, suggesting local flexibility cannot explain our results.

Both modifications resulted in a minimum k_{rel_i} by elongation of the distance between **+2** and **+3** position deoxyribose rings, suggesting that the distance between the deoxyribose rings at positions **+2** and **+3** was more important than the distance between the phosphate groups. Notably, W221 at the position **+3** is known to form the stacking interaction with the deoxyribose ring which is important to prevent the binding of RNA instead of DNA. (Figure 4A).[1] In addition, the distance between the nitrogen atom of Q183 in human RNase H1 and O4´ in deoxyribose at position **+2** was 3.4 Å, indicating the formation of hydrogen bonds. The relative positions of W221 and Q183 in human RNase H1 were well conserved with the corresponding positions of W81 and N45, respectively, in E. coli RNase H (Figure S3B). Thus, the extended distance between these deoxyriboses, **+2** and **+3**, may possibly inhibit DNA recognition, resulting in RNase H-mediated cleavage being significantly suppressed.

Next, we measured RNase H-mediated cleavage patterns of the ASO/**MM** duplexes (Figure 5). The GT mismatched base pair inhibited the cleavage reaction to form ***a*** and ***b*** in all ASOs (Figure 5A) compared to experiments that used fully complementary RNA (Figure 2A). Although ***a*** and ***b*** cleavage products were not observed, cleavage product ***c*** in **3′-HMT-5** was suppressed in a manner identical to that of the **3′-HMT-5**/**PM** duplex. This result suggested that the k_{rel_i} derived from the ASO/**PM** duplex may be used to predict the cleavage patterns of ASO/**MM** duplexes. We hypothesized that k_{rel_i} represents the enhancement or suppression of RNase H-mediated cleavage when the modification is at the *i*-th position. Thus, the cleavage pattern of the modified ASO/**MM** duplex could be calculated from k_{rel_i}, and the cleavage pattern observed in the control/**MM** duplex, if k_{rel_i} of **MM** cleavage is identical to that of **PM** cleavage (Figure 5B). Under this assumption, the fraction of cleavage product obtained when modification occurs at the *i*-th position in the RNase H-ASO/**MM** complex ($p_{m\_i(mm)}$) may be expressed by the following equation (derivation is presented in Supporting Information).

$$p_{m\_i(mm)} = \frac{k_{rel\_i} \cdot p_{c\_i(mm)}}{\sum_i k_{rel\_i} \cdot p_{c\_i(mm)}}$$

where $p_{c\_i\ (mm)}$ is the cleavage product fraction obtained using the control corresponding to $p_{m\_i(mm)}$. The calculated cleavage product fraction at the i-th position ($p_{m\_i(mm)}$) was then converted to the corresponding cleavage product fraction (p_a, p_b, p_c, p_d, or p_e) using the relationship shown (Figure 4A). For example, in the case of **5′-HMT-2**, $p_{m\_0(mm)}$ is the fraction of the product generated by cleavage of mismatched RNA when modification occurred at position **0**, which corresponds to the fraction of cleavage product of ***d*** (p_d). Observed and predicted values are shown (Figure S4). The predicted fractions correlated well with the corresponding observed values (R^2=0.85; Figure 5C). This result suggested that the effect of methylene insertion into the phosphate backbone and the effect of the GT mismatched base pair on RNase H-mediated cleavage were independent.

We also examined the applicability of k_{rel_i} to the cleavage products obtained by mouse Cxcl12 targeting ASO, which is known to show multiple cleavage products.[14] The synthesized ASOs were **Cxcl12-control**, **Cxcl12-5′-HMT**, and **Cxcl12-3′-HMT**, whose sequences were 5′-GCAtgttcXcacaTTA, where X represented thymidine, 5′-HMT, and 3′-HMT, respectively (Figure S5). **Cxcl12-control** was expected to produce six cleavage products, named ***a***, ***b***, ***c***, ***d***, ***e***, and ***f***. By introduction of modification at the middle of gap region, these cleavage products are corresponding to the **0**, **+1**, **+2**, **+3**, **+4**, **+5** position in the RNase H-DNA/RNA complex which is expected to show strong inhibitory effect suggesting by Figure 4B and 4C. For the RNase H cleavage experiment, we used only one-eighth of the RNase H that was used for the HTT targeting experiment, because this RNA was completely cleaved under the same conditions as that used for the HTT experiment. In the case of **Cxcl12-3′-HMT** (X = 3′-HMT), cleavage product ***c***, which

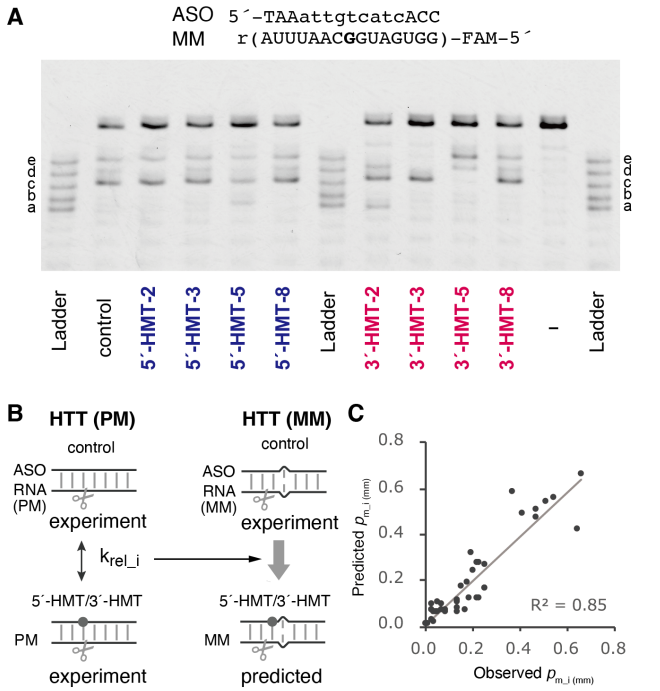

Fig. 5 RNase H-mediated cleavage patterns of ASO/**MM** duplexes. (A) Electrophoretic mobility shift assay of RNase H mediated cleavage products. The cleavage pattern changed depending on the modification as well as the modified position. For the ladder lanes, a mixture of synthetic FAM-labelled RNAs (***a***, ***b***, ***c***, ***d***, and ***e***) was used. (B) Prediction scheme of the cleavage pattern. (C) Correlation of observed values (averaged values from three independent experiments) and predicted values.

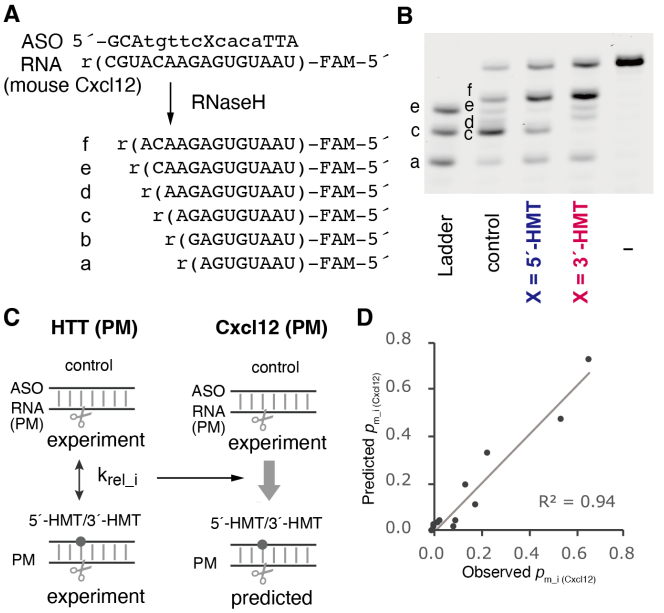

Fig. 6 (A) RNase H-mediated cleavage patterns of Cxcl12 targeting ASO with corresponding complementary RNA. (B) Electrophoretic mobility shift assay of RNase H mediated cleavage products. For the ladder lanes, a mixture of synthetic FAM-labelled RNAs (***a***, ***c***, and ***e***) was used. (C) Prediction scheme of the cleavage pattern. (D) Correlation of observed values (averaged values from three independent experiments) and predicted values.

corresponded to the cleavage product obtained with 3′-HMT at position **+2**, was reduced. Similarly, in **Cxcl12-5′-HMT** (X = 5′-HMT), the cleavage product ***d***, which corresponded to the cleavage product obtained with 5′-HMT at position **+3**, was reduced. To quantitatively compare the results of Cxcl12 ASOs with those observed for HTT ASOs, the cleavage product fractions were predicted using k_{rel_i}, determined by HTT ASOs (Figure 6C). The predicted fractions correlated well with the corresponding observed values (R^2=0.92; Figure 6D), suggesting the inhibitory effect by the insertion of a methylene was similar with the HTT experiments.

Our study has a limitation. We assumed that the largest inhibitory effect would be observed when the disruption of the most important interactions. However, there is still a possibility that the sum of smaller inhibitory effects leads to the largest inhibition. In addition, it is known that the chirality of the phosphorothioate backbone affects the reactivity of RNase H-mediated cleavage. In this study, we did not control the chirality of phosphorothioate. We assumed the distribution of chirality at each nucleotide was the same, but it could be possible that there is a bias due to the modifications, which may influence the result. More thorough studies would be needed. Despite these limitations, the 3′-HMT at position **+2** and 5′-HMT at position **+3** were significantly reduced among different sequences and a mismatched duplex, suggesting that the effect exerted by the insertion of a methylene group at the 5′-side of the position to distinguish ribose and deoxyribose on RNase H-mediated cleavage was a ubiquitous mechanism.

Conclusions

We evaluated the effect of inserting a methylene group into the phosphate backbone of the RNase H-mediated cleavage reaction. Overall, cleavage reactivities were comparable or decreased to 60%, depending on the position of the modifications in the ASO. These results were further verified via an analysis of positional modifications in the RNase H-DNA/RNA complex as reflected by the positional relative kinetic constants (k_{rel_i}). The largest suppression of the cleavage reaction was observed when a methylene group was inserted between **+2** and **+3** deoxyribose rings. This effect was observed in a different sequence as well as mismatched duplexes, suggesting the interaction of deoxyriboses with RNase H is more important than that of phosphate groups. Importantly, **+3** position is known to distinguish ribose and deoxyribose via stacking of the W221 residue in RNase H, suggesting that the distance between the **+2** and **+3** deoxyribose rings may play an important role in the recognition of DNA strands. Our results will contribute to the designing of further molecular modifications that improve the selectivity of RNase H-mediated cleavage reactions which allows for the development of allele-specific ASOs.

Data availability

The data supporting the findings of this study are available within the article and in the ESI.

Author Contributions

Conceptualization, Y.M.; Methodology, Y.M., A.T., S.H., S.W. and K.S.; Investigation, Y.M., A.T., S.H. and S.W.; Writing – Original Draft, Y.M.; Writing – Review & Editing, Y.M., A.T. and K.S.; Funding Acquisition, Y.M.; Resources, Y.M. and K.S.

Conflicts of interest

Y.M. and K.S. are the unpaid member of Fastide, inc.

Acknowledgements

This work was supported by a Grant-in-Aid for Scientific Research from the Ministry of Education, Culture, Sports, Science, and Technology, (Grant No. 20H02857, 20K21245, 21H02075) Japan and JST PRESTO "Genome programming" project (Grant No. JPMJPR19K9), Japan. This work was also partially supported from Japan Agency for Medical Research and development (Grant No. 21fk0210089h0001). We thank the Materials Analysis Division, Open Facility Center, Tokyo Institute of Technology, for their support with the MALDI-TOF-MS. We thank the Open Research Facilities for Life Science and Technology, Tokyo Institute of Technology, for their support with the NMR.

References

1 M. Hyjek, M. Figiel and M. Nowotny, *DNA Repair* , 2019, **84**, 102672.
2 S. T. Crooke, X.-H. Liang, B. F. Baker and R. M. Crooke, *J. Biol. Chem.*, 2021, **296**, 100416.
3 S. T. Crooke, B. F. Baker, R. M. Crooke and X.-H. Liang, *Nat. Rev. Drug Discov.*, 2021, **20**, 427–453.
4 A. Kilanowska and S. Studzińska, *RSC Adv.*, 2020, **10**, 34501–34516.
5 A. Khvorova and J. K. Watts, *Nat. Biotechnol.*, 2017, **35**, 238–248.
6 W. B. Wan and P. P. Seth, *J. Med. Chem.*, 2016, **59**, 9645–9667.
7 Y. Masaki, A. Maruyama, K. Yoshida, T. Tomori, T. Kishimura and K. Seio, *Bioconjug. Chem.*, 2022, **33**, 272–278.
8 T. Yoshida, K. Morihiro, Y. Naito, A. Mikami, Y. Kasahara, T. Inoue and S. Obika, *Nucleic Acids Res.*, 2022, **50**, 7224–7234.
9 L. K. McKenzie, R. El-Khoury, J. D. Thorpe, M. J. Damha and M. Hollenstein, *Chem. Soc. Rev.*, 2021, **50**, 5126–5164.
10 D. Magner, E. Biala, J. Lisowiec-Wachnicka and R. Kierzek, *Sci. Rep.*, 2017, **7**, 12532.
11 M. Nowotny, S. A. Gaidamakov, R. Ghirlando, S. M. Cerritelli, R. J. Crouch and W. Yang, *Mol. Cell*, 2007, **28**, 264–276.
12 N. Iwamoto, D. C. D. Butler, N. Svrzikapa, S. Mohapatra, I. Zlatev, D. W. Y. Sah, Meena, S. M. Standley, G. Lu, L. H. Apponi, M. Frank-Kamenetsky, J. J. Zhang, C. Vargeese and G. L. Verdine, *Nat. Biotechnol.*, 2017, **35**, 845–851.
13 G. Vasquez, G. C. Freestone, W. B. Wan, A. Low, C. L. De Hoyos, J. Yu, T. P. Prakash, M. E. Østergaard, X.-H. Liang, S. T. Crooke, E. E. Swayze, M. T. Migawa and P. P. Seth, *Nucleic Acids Res.*, 2021, **49**, 1828–1839.

14 M. T. Migawa, W. Shen, W. B. Wan, G. Vasquez, M. E. Oestergaard, A. Low, C. L. De Hoyos, R. Gupta, S. Murray, M. Tanowitz, M. Bell, J. G. Nichols, H. Gaus, X.-H. Liang, E. E. Swayze, S. T. Crooke and P. P. Seth, *Nucleic Acids Res.*, 2019, **47**, 5465–5479.

15 B. A. Anderson, G. C. Freestone, A. Low, C. L. De-Hoyos, W. J. D. Iii, M. E. Østergaard, M. T. Migawa, M. Fazio, W. B. Wan, A. Berdeja, E. Scandalis, S. A. Burel, T. A. Vickers, S. T. Crooke, E. E. Swayze, X. Liang and P. P. Seth, *Nucleic Acids Res.*, 2021, **49**, 9026–9041.

16 Y. Takahashi, K. Sato and T. Wada, *J. Org. Chem.*, 2022, **87**, 3895–3909.

17 B. Vester, A. M. Boel, S. Lobedanz, B. R. Babu, M. Raunkjaer, D. Lindegaard, Raunak, P. J. Hrdlicka, T. Højland, P. K. Sharma, S. Kumar, P. Nielsen and J. Wengel, *Bioorg. Med. Chem. Lett.*, 2008, **18**, 2296–2300.

18 M. E. Østergaard, A. L. Southwell, H. Kordasiewicz, A. T. Watt, N. H. Skotte, C. N. Doty, K. Vaid, E. B. Villanueva, E. E. Swayze, C. F. Bennett, M. R. Hayden and P. P. Seth, *Nucleic Acids Res.*, 2013, **41**, 9634–9650.

19 M. E. Østergaard, J. Nichols, T. A. Dwight, W. Lima, M. E. Jung, E. E. Swayze and P. P. Seth, *Mol. Ther. Nucleic Acids*, 2017, **7**, 20–30.

20 M. B. Danielsen, C. Lou, J. Lisowiec-Wachnicka, A. Pasternak, P. T. Jørgensen and J. Wengel, *Chem. Eur. J.*, 2020, **26**, 1368–1379.

21 H. Ueda and Y. Ueno, *Bioorg. Med. Chem.*, 2022, **60**, 116690.

22 S. Frei, A. K. Katolik and C. J. Leumann, *Beilstein J. Org. Chem.*, 2019, **15**, 79–88.

23 P. I. Pradeepkumar, E. Zamaratski, A. Földesi and J. Chattopadhyaya, *J. Chem. Soc. Perkin Trans. 2*, 2001, 402–408.

24 T. Kofoed, P. B. Rasmussen, P. Valentin-Hansen, E. B. Pedersen, K. Rissanen, W. Shi, S. Styring, C. Tommos, K. Warncke and B. R. Wood, *Acta Chem. Scand.*, 1997, **51**, 318–324.

25 Y. S. Sanghvi, R. Bharadwaj, F. Debart and A. De Mesmaeker, *Synthesis*, 1994, **1994**, 1163–1166.

26 J. B. Carroll, S. C. Warby, A. L. Southwell, C. N. Doty, S. Greenlee, N. Skotte, G. Hung, C. F. Bennett, S. M. Freier and M. R. Hayden, *Mol. Ther.*, 2011, **19**, 2178–2185.

27 H. Wu, W. F. Lima and S. T. Crooke, *J. Biol. Chem.*, 2001, **276**, 23547–23553.

28 R. R. Davis, N. M. Shaban, F. W. Perrino and T. Hollis, *Cell Cycle*, 2015, **14**, 668–673.